Crystallographic Procedures. Crystalline samples suitable for diffraction analysis were obtained as follows. Colorless crystals of **1** were obtained from benzene solution at room temperature. Light-yellow crystals of **2** were obtained from the reaction mixture in benzene at 5 °C. Colorless crystals of **3** and dark-red crystals of **5** were obtained from the respective reaction mixtures at -20 °C. Dark-purple plates of **6**·THF were obtained from the reaction mixture in hexane at room temperature.

All samples were mounted in thin-wall glass capillaries in an inert-atmosphere glovebox. The intensity data for compounds **1**, **3**, and **5** were collected on a Siemens R3m/v diffractometer at ambient temperature. The data for **2** and **6** were collected on a Nicolet P3 diffractometer at ambient temperature. On both diffractometers, Mo Kα radiation (λ = 0.710 73 Å) was used except in the case of **1** for which Cu Kα radiation was used (λ = 1.541 78 Å).

Crystallographic calculations were done on a microVAX II using the Siemens SHELXTL PLUS program package. Crystal data are summarized in Table II. Neutral-atom scattering factors were used.[55] All structures were solved by direct methods. On the basis of systematic extinctions or lack of them, the space groups were assigned to be $P\bar{1}$ (No. 2) for **1-3**, and **6**, and $P2_12_12_1$ (No. 19) for **5**. Refinements for each are described in the supplementary material. All non-hydrogen atoms were refined anisotropically. All hydrogen atoms were placed in calculated positions (d_{C-H} = 0.96 Å) and included in the final structure factor calculations by using a riding model. Final positional parameters are given in the supplementary material.

(55) *International Tables for X-ray Crystallography*; Hahn, T., Ed.; Kynock Press: Birmingham, England, 1974; Vol. IV, pp 99, 149.

Acknowledgment. Funding was provided by the Petroleum Research Fund, administered by the American Chemical Society, and an NSF Presidential Young Investigator award supported by the Monsanto Co. and the Eastman Kodak Co. Washington University's X-ray Crystallography Facility was funded by the NSF Chemical Instrumentation Program (Grant CHE-8811456). The Washington University High-Resolution NMR Service Facility was funded in part by NIH Biomedical Research-Support Shared-Instrument Grant 1 S10 RR02004 and a gift from the Monsanto Co. We thank Dr. Charles Campana from Siemens Analytical X-Ray Instruments, Inc. for collecting the data for compound **1**.

Supplementary Material Available: Tables listing details of the crystallographic data collection, atomic coordinates, bond distances, bond angles, calculated hydrogen atom parameters, and anisotropic thermal parameters (29 pages); listings of observed and calculated structure factors (117 pages). Ordering information is given on any current masthead page.

Complexes with Pt-H-Ag Bonds

Alberto Albinati,[†] Stanislav Chaloupka,[‡] Francesco Demartin,[†] Thomas F. Koetzle,[§] Heinz Rüegger,[‡] Luigi M. Venanzi,*[,‡] and Martin K. Wolfer[‡]

Contribution from the Istituto di Chimica Farmaceutica, Università di Milano, I-20131 Milano, Italy, Chemistry Department, Brookhaven National Laboratory, Upton, New York 11973, and Laboratorium für Anorganische Chemie, ETH-Zentrum, CH-8092 Zürich, Switzerland.
Received May 26, 1992

Abstract: Silver ions react with 2 equiv of the hydrides *trans*-[PtH(C_6X_5)(PR_3)$_2$] (X = F and Cl, R = Me and Et; X = H, R = Et) to give trinuclear complex cations of the type [(PR_3)$_2$(C_6X_5)Pt(μ-H)Ag(μ-H)Pt(C_6X_5)(PR_3)$_2$]$^+$ which were characterized by multinuclear NMR spectroscopy. A full report of the X-ray crystal structure of [(PEt_3)$_2$(C_6Cl_5)Pt(μ-H)Ag(μ-H)Pt(C_6Cl_5)(PEt_3)$_2$](CF_3SO_3) is also given. The silver ion in this complex is linear with two hydride ligands, the H-Ag-H angle being ca. 152°. Significant Pt···Ag direct interactions are also likely to occur. Crystal data: space group $P\bar{1}$, a = 13.853 (3) Å, b = 14.214 (2) Å, c = 15.611 (3) Å, α = 94.64 (2)°, β = 90.48 (2)°, γ = 110.39 (2)°, Z = 2, V = 2869.7 Å^3, ρ(calcd) = 1.875 g cm^{-3}, R = 0.049. The reaction of $AgCF_3SO_3$ and *trans*-[PtH(C_6Cl_5)(PEt_3)$_2$], in a 1:1 ratio, gave the complex [(PEt_3)$_2$(C_6Cl_5)Pt(μ-H)Ag(H_2O)](CF_3SO_3), which was characterized by multinuclear NMR spectroscopy and by X-ray and neutron diffraction. Also in this complex, the silver ion is linearly coordinated. Here, however, it is bonded to one hydride ligand and to one water molecule. Crystal data (neutron, 24 K): space group $P\bar{1}$, a = 8.581 (2) Å, b = 12.053 (3) Å, c = 15.519 (3) Å, α = 87.86 (2)°, β = 73.55 (2)°, γ = 81.76 (2)°, Z = 2, V = 1523 Å^3, ρ(calcd) = 2.105 g cm^{-3}, $R(F^2)$ = 0.081.

Introduction

The affinity of the silver ion for transition metal hydride complexes is now well documented.[1] A general feature of these compounds is the strength of the L_nMH_x·AgL′ interaction.[2] One of the most remarkable classes of compounds with this type of interaction contains a silver ion bonded to two *trans*-[PtH(R)(PR'_3)$_2$] units,[3] with the structure shown schematically as follows:

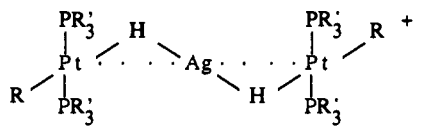

We report here the full characterization of compounds of this type as well as the X-ray and neutron diffraction structures of the related bimetallic compound [(PEt_3)$_2$(C_6Cl_5)Pt(μ-H)Ag(H_2O)](CF_3SO_3).

Results and Discussion

The Trimetallic Pt-H-Ag-H-Pt Complexes. As reported earlier, cationic species of the type [(PR_3)$_2$(C_6X_5)Pt(μ-H)Ag(PR'_3)]$^+$[4] (**1**) disproportionate in solution as shown in eq 1.

$$2[(PR_3)_2(C_6X_5)Pt(\mu\text{-}H)Ag(PR'_3)]^+ \rightleftharpoons \underset{\mathbf{1}}{[(PR_3)_2(C_6X_5)Pt(\mu\text{-}H)Ag(\mu\text{-}H)Pt(C_6X_5)(PR_3)_2]^+} + \underset{\mathbf{2}}{[Ag(PR'_3)_2]^+} \quad (1)$$

[†] Università di Milano.
[‡] ETH-Zentrum.
[§] Brookhaven National Laboratory.

(1) Albinati, A.; Anklin, C.; Janser, P.; Lehner, H.; Matt, D.; Pregosin, P. S.; Venanzi, L. M. *Inorg. Chem.* **1989**, *28*, 1105 and references quoted therein.
(2) Braustein, P.; Gomes Carneiro, T. M.; Matt, D.; Tiripicchio, A.; Tiripicchio Camellini, M. *Angew. Chem., Int. Ed. Engl.* **1986**, *25*, 748.
(3) Albinati, A.; Demartin, F.; Venanzi, L. M.; Wolfer, M. K. *Angew. Chem., Int. Ed. Engl.* **1988**, *27*, 563.

0002-7863/93/1515-169$04.00/0

Table I. NMR Data for *trans*-$[PtH(C_6X_5)(PR_3)_2]$ (**3**), $[(PR_3)_2(C_6X_5)Pt(\mu\text{-}H)Ag(\mu\text{-}H)Pt(C_6X_5)(PR_3)_2]^+$ (**2**), and $[(PEt_3)_2(C_6Cl_5)Pt(\mu\text{-}H)Ag(H_2O)]^+$ (**5e**)[a]

R	X	complex	δ(H) (ppm)	^1J(Pt,H) (Hz)	^1J(Ag,H)[b] (Hz)	δ(P) (ppm)	^1J(Pt,P) (Hz)	^3J(Ag,P) (Hz)	temp (K)
Me	F	**3a**	−7.30	833		−13.3	2540		room temp
Me	F	**2a**	−6.5	650	110[b]	−19.9	2256	n.o.	163
Me	Cl	**3b**	−9.06	780		−21.9	2653		room temp
Me	Cl	**2b**	−7.65	598	113/131[c]	−20.9	2240	5.7	183
Et	H	**3c**	−7.05	648		17.3	2797		room temp
Et	H	**2c**	−5.86	527	122/141[c]	17.9	2450	3.5[d]	203
Et	F	**3d**	−7.88	787		17.6	2682		room temp
Et	F	**2d**	−6.45	623	120[b]	18.1	2171	n.o.	183
Et	Cl	**3e**	−9.80	729		15.9	2772		room temp
Et	Cl	**2e**	−7.97	570	115/134[c]	11.4	2290	4.2[e]	233
Et	Cl	**5e**	−8.75	625	*f*/171[g]	10.9	2322	n.o.	203
Et	Cl	**5e**[h]	−8.32	585	111/127[c]	10.7	2361	n.o.	188

[a] Spectra were recorded in CD_2Cl_2 unless otherwise stated. [b] Separate signals due to each isotopomer were not observed. [c] The first value refers to ^{107}Ag. [d] δ(^{109}Ag) = 503 ppm; ^2J(Pt,^{109}Ag) = 390 Hz; ^3J(Pt,H) = 35 Hz. [e] δ(^{109}Ag) = 431 ppm; ^2J(Pt,^{109}Ag) = 544 Hz; δ(^{195}Pt) = −4811 ppm. [f] Not obtained. [g] δ(^{109}Ag) = 284 ppm; ^2J(Pt,^{109}Ag) = 739 Hz; δ(^{195}Pt) = −4869 ppm. [h] In acetone-d_6.

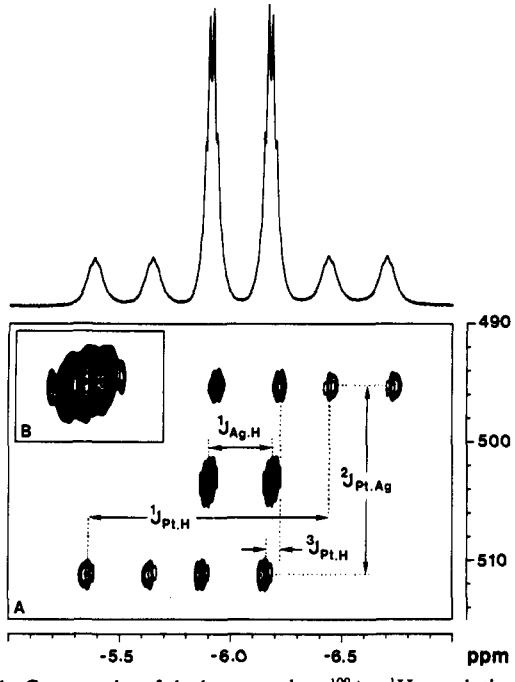

Figure 1. Contour plot of the heteronuclear ^{109}Ag–^{1}H correlation spectrum (23.3–500.13 MHz) of $[(PEt_3)_2(C_6H_5)Pt(\mu\text{-}H)Ag(\mu\text{-}H)Pt(C_6H_5)(PEt_3)_2]^+$ (**2c**) recorded in CD_2Cl_2 solution at 213 K. One of the central resonances is shown expanded in the insert (B), and the hydride region of the conventional ^{1}H spectrum is plotted on top. Atom symbols refer to the isotopes ^{195}Pt, ^{109}Ag, and ^{1}H.

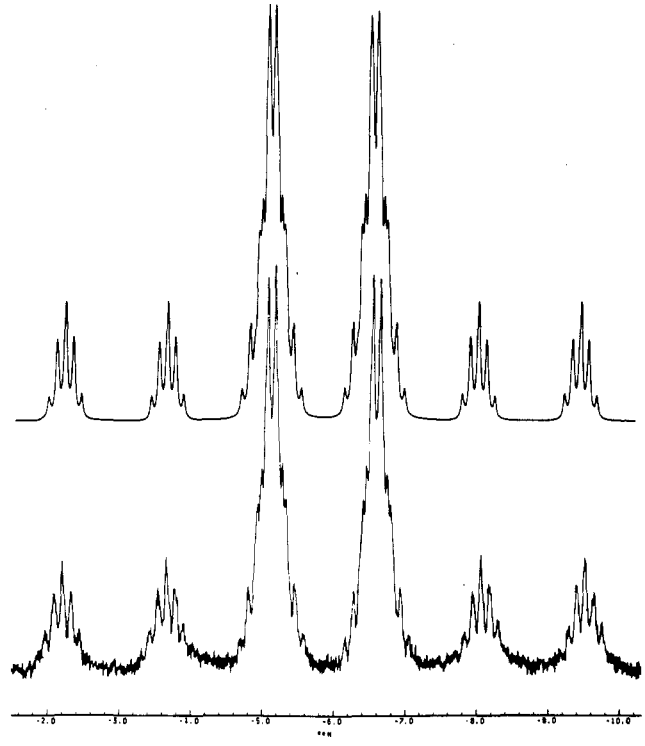

Figure 2. (a, Bottom) Hydride region of the 90-MHz ^{1}H NMR spectrum (acetone-d_6, −70 °C) of $[(PEt_3)_2(C_6H_5)Pt(\mu\text{-}H)Ag(\mu\text{-}H)Pt(C_6H_5)(PEt_3)_2]^+$ (**2c**). (b, Top) PANIC simulation of the experimental spectrum below (the parameters used are listed in Table I).

Compounds containing cations of type **2** can be directly obtained by reacting 2 equiv of the mononuclear complexes of the type *trans*-$[PtH(C_6X_5)(PR_3)_2]$ (**3**) with 1 equiv of silver ion, e.g., in the form of its triflate. The compounds prepared and some relevant NMR data are summarized in Table I.

Multinuclear NMR studies of these complex cations allow unambiguous structural assignments of the molecular geometries of the complexes in solution. While the triplet multiplicity of the silver resonance caused by the two coordinated hydrides can be derived from either an INEPT[5] or a DEPT[6] spectrum, the most informative spectrum consists of the ^{109}Ag–^{1}H heteronuclear correlation[7] performed for, e.g., $[(PEt_3)_2(C_6H_5)Pt(\mu\text{-}H)Ag(\mu\text{-}H)Pt(C_6H_5)(PEt_3)_2]^+$ (**2c**), shown in Figure 1. In addition to the main resonances visible in the center of the contour plot, one easily recognizes two sets of platinum satellites, each separated by the silver–proton coupling constant. The latter signals arise from the one- and three-bond platinum–proton couplings, respectively, and thus confirm the trimetallic nature of the compound. Furthermore, an expansion of one of the central resonances (see Figure 1, insert B) shows a quintetlike multiplicity due to the four phosphorus spins of the PEt_3 ligands.

In addition to the structural information contained in this spectrum, one should also note that the reduced coupling constants ^1K(^{195}Pt,^{1}H) and ^3K(^{195}Pt,^{1}H) have the same sign whereas ^2K(^{195}Pt,^{109}Ag) has the opposite sign. Assuming a positive sign for ^1K(^{195}Pt,^{1}H), which is generally the case,[8] the constant ^nK(^{195}Pt,^{109}Ag) is likely negative. The latter constant could be formally described as ^1K if one considers only the Pt–Ag direct bond or as ^2K if this coupling occurs through a Pt–H–Ag pathway. A combination of the two is also conceivable. The observation

(4) Albinati, A.; Lehner, H.; Venanzi, L. M.; Wolfer, M. K. *Inorg. Chem.* **1987**, *26*, 3933.
(5) Morris, G. A.; Freeman, R. *J. Am. Chem. Soc.* **1979**, *101*, 760.
(6) Bendall, M. R.; Doddrell, D. M.; Pegg, D. T. *J. Am. Chem. Soc.* **1981**, *103*, 4603.
(7) Summers, M. F.; Marzilli, L. G.; Bax, A. *J. Am. Chem. Soc.* **1986**, *108*, 4285.
(8) Pregosin, P. S. In *Transition Metal Nuclear Magnetic Resonance*; Pregosin, P. S., Ed.; Studies in Inorganic Chemistry, Vol. 13; Elsevier: New York, 1991; p 216 and references quoted therein.

Table II. ν(Pt-H) and ν(Pt-H-Ag) Frequencies (cm^{-1}) for *trans*-$[PtH(C_6X_5)(PR_3)_2]$ (**3**) and $[(PR_3)_2(C_6X_5)Pt(\mu\text{-}H)Ag(\mu\text{-}H)Pt(C_6H_5)(PR_3)_2]^+$ (**2**)[a]

R	X	complex	ν(Pt-H)	complex	ν(Pt-H-Ag)
Me	F	**3a**	2010	**2a**	1697
Me	Cl	**3b**	2008	**2b**	1679
Et	F	**3d**	2039	**2d**	~1700[b]
Et	Cl	**3e**	2018	**2e**	1696

[a] Spectra were recorded for CH_2Cl_2 solutions. [b] Because of the presence of several low- to medium-intensity bands in the region 1600–1800 cm^{-1} due to the organic part of the molecule, clearly visible in the spectrum of the mononuclear complex **3d**, it is not possible to give an accurate maximum for this band: the apparent value in CH_2Cl_2 solution is 1628 cm^{-1}, while that in Nujol is 1714 cm^{-1}.

of a negative sign might be valuable for the understanding of the electronic structure of the molecule as it points out that the geminal coupling pathway via the hydridic bridge contributes significantly more to the silver–platinum coupling constant than the direct metal–metal interaction. This is consistent with the description of the bonding presented later.

The ^1H NMR spectra in the hydride region are quite complex, as can be seen in Figure 2, which shows the resonances arising from the two hydride ligands in $[(PEt_3)_2(C_6H_5)Pt(\mu\text{-}H)Ag(\mu\text{-}H)Pt(C_6H_5)(PEt_3)_2]^+$ (**2e**). However, as shown also in Figure 2, this spectrum can be successfully simulated using the parameters listed in Table I. Two main trends are apparent here: hydride coordination to silver (1) shifts the $\delta(^1H)$ values to lower fields and (2) reduces the values of the $^1J(^{195}Pt,^1H)$ coupling constants. Similar effects have been observed in the related compounds $[(PR_3)_2(C_6Cl_5)Pt(\mu\text{-}H)Ag(PR'_3)]^{+4}$ (**1**) as well as in other hetero- and even homonuclear hydrido-bridged complexes.[1] These changes have been interpreted in terms of a weakening of the Pt–H bond upon coordination to a Lewis acid, Ag^+ in this case.

The presence of the ^{107}Ag and ^{109}Ag isotopes in complex cations of type **2** does not always lead to the observation of splittings due to each isotopomer. This is particularly the case for spectra recorded at high B_0 field strengths; e.g., compare the projection in Figure 1 (11.4 T) with the spectrum in Figure 2 (2.1 T). However, when these are observed, the ratios of the coupling constants correspond to the magnetogyric ratios of the two isotopes. The values of the ^1J(Ag,H) coupling constants (110–140 Hz) are somewhat larger than those recorded for the related complexes of the type $[(PR_3)(C_6Cl_5)Pt(\mu\text{-}H)Ag(PR'_3)]^+$ (**1**) (80–100 Hz). The higher J values for the complexes of type **2** could be a consequence of stronger Ag–H interactions in these compounds. This would be consistent with the expectations that "$\{PtH(C_6X_5)(PR_3)_2\}Ag^+$" is a stronger Lewis acid than "$(PR_3)Ag^+$", as tertiary phosphines are expected to be better electron donors than the hydride ligand in *trans*-$[PtH(C_6X_5)(PR_3)_2]$.

However, the ^1J(Ag,H) values in the trinuclear complex cations of type **2** are comparable with $^1J(Ag,H^1)$ constants found in complexes of type **4** (112–116 Hz).[1] It is noteworthy that J-

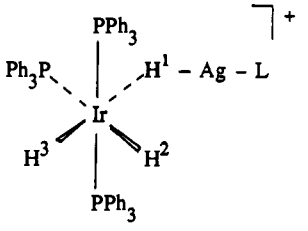

4a; L = PPh_3

4b; L = PEt_3

(Ag,H^2) values for the two cations **4a** and **4b** are 23 and 24 Hz, respectively, while the corresponding $J(Ag,H^3)$ values are even smaller (12 and 15 Hz, respectively).

Little additional information is obtainable from the ^{31}P NMR data, also given in Table I. As found in related compounds, there is a systematic decrease in the values of the $^1J(^{195}Pt,^{31}P)$ coupling constants on adding the "Lewis acid" to the hydride complex, while the changes in $\delta(^{31}P)$ are more random.[1]

The infrared stretching vibrations involving the "Pt–H" and "Pt–H–Ag" moieties are listed in Table II. While the ν(Pt-H) vibration in the mononuclear complexes occurs as a sharp band between 2008 and 2039 cm^{-1}, in the trimetallic complexes the band is replaced by a broad feature at ca. 1700 cm^{-1}. These changes are consistent with the postulated structures.[9] It was also observed that the ν(Pt–H) vibrations of the monometallic species, **3**, were ca. 10 cm^{-1} higher in Nujol than in CH_2Cl_2, while the converse was true for the trimetallic cations, **2**.

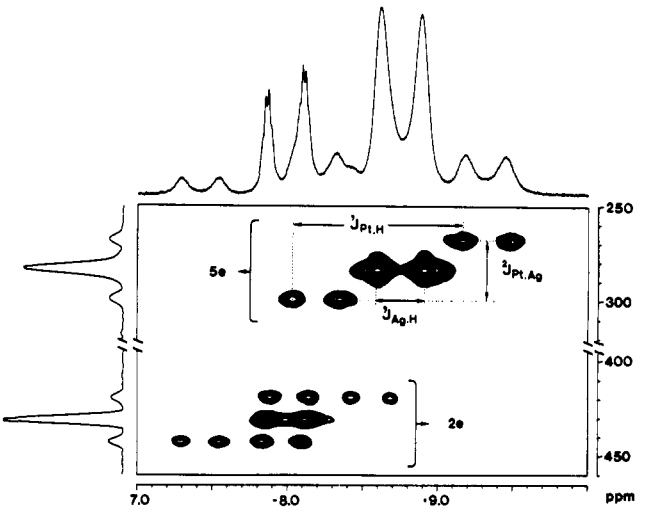

Figure 3. Contour plot of the heteronuclear ^{109}Ag–^1H correlation spectrum (23.3–500.13 MHz) of $[(PEt_3)_2(C_6Cl_5)Pt(\mu\text{-}H)Ag(\mu\text{-}H)Pt(C_6Cl_5)(PEt_3)_2]^+$ (**2e**) and $[(PEt_3)_2(C_6Cl_5)Pt(\mu\text{-}H)Ag(OH_2)]^+$ (**5e**) recorded in CD_2Cl_2 solution at 203 K. The hydride region of the conventional ^1H spectrum is shown on top, whereas the ^{109}Ag spectrum to the left resulted from a projection of the 2D peaks onto the ω_1 axis. (For an interpretation of the signals for **2e** and the meaning of the atom symbols, see Figure 1.)

Finally, mention should be made of the relative stabilities of these compounds. Particularly evident is their photosensitivity which is most marked in the phenyl compound **2c**. It is also observed that the PMe_3 complexes in this respect appear to be somewhat more sensitive than those with PEt_3. However, no significant differences are observed between corresponding C_6F_5 and C_6Cl_5 compounds. Similar trends are observed for the thermal stabilities. However, all the compounds except [**2c**](CF_3SO_3) are air-stable.

The observation that the lowest photosensitivity is shown by the compounds containing the more electron-withdrawing aryl substituents, i.e., C_6F_5 and C_6Cl_5, could be taken as an indication that the formation of metallic silver from photodecomposition is caused by electron transfer involving an orbital having mainly hydridic character: the lower the energy of this orbital relative to the silver acceptor orbital, the more difficult the electron-transfer process.

The Bimetallic Pt–H–Ag–OH_2 Complex. When the complex *trans*-$[PtH(C_6Cl_5)(PEt_3)_2]$, dissolved in reagent grade Et_2O, was treated with 1 equiv of $AgCF_3SO_3$, the colorless complex cation $[(PEt_3)_2(C_6Cl_5)Pt(\mu\text{-}H)Ag(H_2O)](CF_3SO_3)$ (**5e**) was formed. The IR spectrum of this solid showed a broad band at 1709 cm^{-1} (in Nujol) consistent with the presence of a "Pt–H–Ag" unit. The NMR spectra, recorded in CD_2Cl_2 solution, indicate the occurrence of the equilibria shown in eqs 2 and 3 (for a definition of

$$2[(PEt_3)_2(C_6Cl_5)Pt(\mu\text{-}H)Ag(H_2O)]^+ + (x-2)H_2O \rightleftharpoons \underset{\textbf{5e}}{} [(PEt_3)_2(C_6Cl_5)Pt(\mu\text{-}H)Ag(\mu\text{-}H)Pt(C_6Cl_5)(PEt_3)_2]^+ + \underset{\textbf{2e}}{} Ag(H_2O)_x^+ \quad (2)$$

$$[(PEt_3)_2(C_6Cl_5)Pt(\mu\text{-}H)Ag(H_2O)] + Ag^*(H_2O)_x^+ \rightleftharpoons [(PEt_3)_2(C_6Cl_5)Pt(\mu\text{-}H)Ag^*(H_2O)]^+ + Ag(H_2O)_x^+ \quad (3)$$

(9) Cooper, C. B.; Shriver, D. F.; Onaka, S. In *Transition Metal Hydrides*; Bau, R., Ed.; Advances in Chemistry Series 167; American Chemical Society: Washington, DC, 1978; p 232.

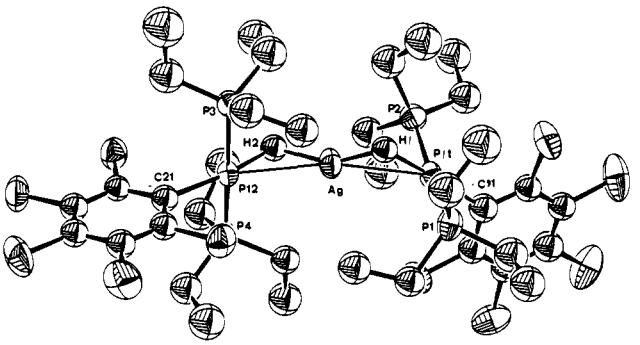

Figure 4. ORTEP drawing of the cation $[(PEt_3)_2(C_6Cl_5)Pt(\mu\text{-}H)Ag(\mu\text{-}H)Pt(C_6Cl_5)(PEt_3)_2]^+$ (**2e**).

Ag*, see footnote 10). At room temperature, one observes only one set of broad hydride resonances, lacking silver couplings; at lower temperature, e.g., at 203 K, one registers two distinctive patterns which, on the basis of the ^{109}Ag-^1H heteronuclear correlation spectrum shown in Figure 3, can be assigned to the trimetallic complex **2e** and the bimetallic species **5e**, respectively. While the values of the parameters of the bimetallic complex directly involving the silver nucleus, e.g., $\delta(^{109}Ag)$ = 284 ppm, $^2J(^{195}Pt,^{109}Ag)$ = 739 Hz, and $^1J(^{109}Ag,^1H)$ = 171 Hz are remarkably different from the corresponding values of the trimetallic compound $\delta(^{109}Ag)$ = 431 ppm, $^2J(^{195}Pt,^{109}Ag)$ = 554 Hz, and $^1J(^{109}Ag,^1H)$ = 146 Hz, those restricted to the fragment $\{(PEt_3)_2(C_6Cl_5)PtH\}$ are quite similar. The equilibrium decribed in eq 2 can be shifted toward the trimetallic species **2e** by using CD_2Cl_2 saturated with water as the solvent or, alternatively, toward the bimetallic cation **5e** by the addition of solid silver triflate. In the latter case, at room temperature, one observes for the hydride a sharp triplet with additional platinum satellites due to coupling to two equivalent phosphorus atoms and the platinum, respectively, whereas the coupling to $^{107}Ag/^{109}Ag$ is completely lost. This observation is consistent with a fast exchange, on the NMR time scale, of the silver ions as indicated in eq 3. At low temperature, 183 K, a static situation is reached, showing mainly the bimetallic complex and only a small amount of the trimetallic species.

Although the above NMR data do not indicate the presence of a molecule of water coordinated to silver in solution, its presence, at least in the solid state, is demonstrated by the neutron diffraction studies described later.

While the coordinated water molecule in $[\mathbf{5e}](CF_3SO_3)$ obviously originated from the quality of the solvent used, it is noteworthy that bands due to the aquo complex of type **5** were also observed when the IR spectra of the trimetallic complexes **2** were not recorded under strictly anhydrous conditions. The formation of these compounds may be taken as an indication of the preference of the silver ion to coordinate water rather than the platinum hydrides of type **3**.

X-ray Crystal Structure of $[(PEt_3)_2(C_6Cl_5)Pt(\mu\text{-}H)Ag(\mu\text{-}H)Pt(C_6Cl_5)(PEt_3)_2](CF_3SO_3)$ ($[\mathbf{2e}](CF_3SO_3)$). As pointed out in a preliminary communication,[3] the X-ray crystal structure of this compound shows it to be a hydrido-bridged trimetallic complex. A list of interatomic distances and angles is obtainable as indicated in ref 3, and an ORTEP view of the cation is shown in Figure 4.

The trimetallic unit is approximately linear (ca. 166°). The two *trans*-$[PtH(C_6Cl_5)(PEt_3)_2]$ square-planar units, flanking the silver atom, define an angle of 83.5° between the two platinum coordination planes. The positions of the hydride ligands could be located on the difference Fourier map (see Experimental Section), the average of the Pt-H as well as the Ag-H distances being 1.7 (1) Å. Given the high standard deviations, these values fall in the range observed for Pt-H and Ag-H in $[(PEt_3)_2(C_6Cl_5)Pt(\mu\text{-}H)Ag(H_2O)](CF_3SO_3)$ ($[\mathbf{5e}](CF_3SO_3)$), (for which

(10) The Ag^+ and Ag^{*+} ions, in the left-hand side of eq 3 denote a silver ion bonded to the platinum hydride and a solvated ion in solution, respectively, undergoing exchange.

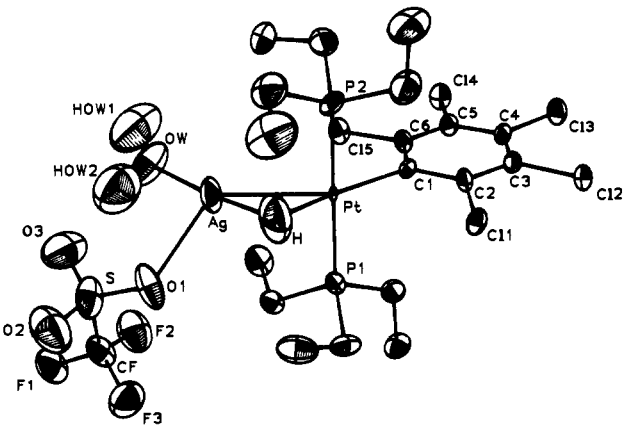

Figure 5. ORTEP drawing of the cation $(PEt_3)_2(C_6Cl_5)Pt(\mu\text{-}H)Ag(OH_2)]^+$ (**5e**) obtained by neutron diffraction.

neutron diffraction data are available (see later). The other structural parameters, i.e., those concerning Pt-P and Pt-C bonds, are normal for compounds containing the Pt-H-M unit[4] and need no further comment.

The most remarkable feature of compounds of type **2** is the stability of the hydrido-bridged trimetallic unit. If one describes it as resulting from two Pt-H-Ag three-center two-electron interactions, taking as a basis the now familar "donor-acceptor" scheme,[11] one cannot fail to be astonished by the resulting stability of the silver ion in this type of coordination. The single Pt-H-Ag interaction in the related compounds $[(PR_3)(C_6X_5)Pt(\mu\text{-}H)Ag(PR'_3)]^+$ (**1**) is more easily rationalized given the presence of the PR'_3 ligand coordinated to silver. However, the formation of a stable molecular compound in which the electronic requirements of the silver ion are satisfied by only two three-center two-electron bonds is difficult to conceive. A possible explanation for the stability of the Pt-H-Ag-H-Pt moiety is provided by the small Pt-H-Ag angle (106 (4)° average), which is characteristic for "closed" M-H-M' interactions.[12] This implies a significant direct M-M' bonding consistent with the observed Pt-Ag distance (2.791 (1) Å) and suggests an alternative description of the bonding in the Pt-H-Ag-H-Pt central unit in terms of (1) two Pt-Ag σ-bonds, each resulting from the overlap of one digonal hybrid orbital of the silver atom with one filled nonbonding platinum d-orbital of the square-planar monometallic unit, and (2) two three-center two-electron bonds, each involving the orbitals forming the Pt-H σ-bonds and an empty p-type orbital of the silver atom (if one defines the z-axis as that of the Pt-Ag-Pt direction, this would be either p_x or p_y), the two electrons for each three-center bond being those of the Pt-H bond. This interaction would place the two Pt-H-Ag planes orthogonal to one another as found.

This description, although analogous to that given earlier[3] based on the formation of only two three-center two-electron bonds, has the advantage of stressing the formation of stronger Pt-Ag bonds and of involving all the 5s and 5p Ag orbitals in the trimetallic interaction, leading to greater electron delocalization.

Crystal Structure of $[(PEt_3)_2(C_6Cl_5)Pt(\mu\text{-}H)Ag(H_2O)](CF_3SO_3)$ ($[\mathbf{5e}](CF_3SO_3)$). This was determined at room temperature by X-ray and at low temperature by neutron diffraction. The latter results will be discussed first, given their greater accuracy. The few significant differences between the two sets of structural parameters will be commented upon later. A list of bond lengths and angles is given in supplementary Table S1, and an ORTEP drawing of the compound is shown in Figure 5.

The solid-state structure of this compound consists of a square-planar *trans*-$[PtH(C_6Cl_5)(PEt_3)_2]$ complex sharing a hydride ligand with an approximately linear "HAg{O(W)}" unit. This oxygen atom, that of the water molecule coordinated to silver,

(11) Venanzi, L. M. *Coord. Chem. Rev.* **1982**, *43*, 251 and references quoted therein.

(12) (a) Bau, R.; Teller, R. G.; Kirtley, S. W.; Koetzle, T. F. *Acc. Chem. Res.* **1979**, *12*, 176. (b) Teller, R. G.; Bau, R. *Struct. Bonding (Berlin)* **1981**, *44*, 1.

deviates only slightly (0.05 Å) from the plane defined by the C(1)-Pt-H-Ag atoms. The coordination environment at the silver atom is completed by one of the CF_3SO_3 oxygen atoms, O(1), resulting in a T-shaped geometry. This and the long Ag-O(1) distance (2.471 (3) Å) are indicative of a mainly electrostatic interaction between Ag and O(1).

The T-shaped arrangement of the donor atoms around silver has been previously observed in complexes coordinated to two phosphorus atoms and one weakly held oxygen donor, i.e., [Ag-Y(PP)] (Y = NO_3 or ClO_4; PP = 2,11-bis((diphenylphosphino)methyl)benzo[*c*]phenanthrene), where P-Ag-P angles between 149 and 169° and Ag-O distances between 2.48 and 3.22 Å have been reported.[13,14]

The bond lengths and angles of the non-hydrogen atoms in the square-planar Pt-H-C(1)-P(1)-P(2) unit are very similar to those found in analogous mono- and binuclear hydrido complexes.[4,15] The Pt-Ag distance (2.750 (3) Å) is not unusual for this type of compound, being comparable with the Ir-Ag distance in $[(PPh_3)_3H_2Ir(\mu\text{-}H)Ag(PPh_3)]^+$ (2.758 (2) Å), the Ir-Au distance in $[(PPh_3)_3H_2Ir(\mu\text{-}H)Au(PPh_3)]^+$[1] (2.765 (1) Å), and the Pt-Au distance in $[(PEt_3)_2(C_6F_5)Pt(\mu\text{-}H)Au(PPh_3)]^+$[4] (**6**) (2.714 (1) Å). It should also be noticed that the Ag-H-Pt angle in compound **5e** (103.3 (2)°) and the Au-H-Pt angle in compound **6a** (103 (4)°) indicate that the M-H-M′ interactions in the two compounds are similar. These data also support the assumption, made in a previous publication,[4] that short M-M′ distances are associated with small M-H-M′ angles.

Also in the case of compound **5e**, the Pt-H-Ag interaction can be described using the usual three-center two-electron scheme,[12] the Pt-H-Ag angle of 103.3 (2)° together with the near linearity of H-Pt-C(1) and H-Ag-O(W) clearly indicating that this interaction must be described as "closed".

The Pt-H distance (1.674 (4) Å) is shorter than the Ag-H distance (1.831 (5) Å), as would be expected on the basis of the radii of the two metal atoms. As the use of standard radii would pose problems in this case, the relative "atomic" sizes of the two metals in environments similar to those found in **5e** were obtained by comparing the Pt-P distance in *trans*-$[PtH(C_6H_5)(PEt_3)_2]$ (2.271 (4) Å)[15] with Ag-P in $[Ag(ClO_4)(PP)]$ (2.405 (3) Å). The latter compound was chosen as it contains a nearly linear P-Ag-P unit interacting fairly weakly with one oxygen atom on the perchlorate anion. On the basis of the above data, one would deduce that the "Ag radius" is ca. 0.13 Å longer than the "Pt radius", in reasonable agreement with the observed Pt-H and Ag-H distances in **5e**.

Finally, the Ag-O(W) distance (2.259 (4) Å) in compound **5e** falls in the normal range of Ag-O distances[13] and is also comparable with that in the related compound $[(PPh_3)IrH_3Ag_2(H_2O)](CF_3SO_3)_2$ (2.23 (3) Å).[3] The H-O-H angle in **5e** is practically the same as that in gaseous H_2O (104.50°), as are the O-H distances (0.9724 Å).[16]

The orientation of H_2O relative to silver is likely to be determined by the hydrogen bonds formed, one of them being intramolecular between H(2) and O(3), i.e., the triflate oxygen directly associated with the cation, and the other being intermolecular, i.e., between H(1) and an O(2) belonging to a neighboring triflate related to the former through the center of symmetry.

To our knowledge, the low-temperature neutron data provide, for the first time, an accurate geometry for the triflate anion, which is usually disordered at room temperature in coordination compounds.

The most significant differences between the X-ray and neutron structural data are mainly concerned with the coordination around the silver ion and in particular the Pt-Ag and Ag(OW) distances. These differences can be attributed to disorder of the silver ion as deduced from its high thermal factors, which are 7.3 $Å^2$ at room temperature and 3.0 $Å^2$ at 24 K. (See also supplementary Tables S2 and S3.) This disorder must be, at least in part, of static nature as the neutron diffraction data collected at 24 K still show a mean-square displacement of the silver atom larger than that expected on the basis of the observed decreases of the thermal factors of other atoms, e.g., P or Pt.

The differences in parameters involving the triflate anion are also attributable to disorder at room temperature.

Experimental Section

All manipulations were performed in Schlenk-type flasks under purified nitrogen and under light exclusion. Unless otherwise stated, the solvents, of grade "puriss, p.a." purchased from Fluka AG, were used without further treatment. Infrared spectra in the region 4000–400 cm^{-1} were recorded on a Perkin-Elmer Model 883 spectrophotometer as CH_2Cl_2 solution or Nujol mulls. The ^1H, $^{31}P\{^1H\}$, and $^{195}Pt\{^1H\}$ NMR spectra were recorded using Bruker HX-90, WH-90, WM-250, AM-300, and AM-400 spectrometers. Inverse $^{109}Ag-^1H$ correlation spectra were measured on a Bruker AMX-500 instrument operating at 500.13 and 23.3 MHz for ^1H and ^{109}Ag, respectively. The following references were used: ^1H, TMS; ^{31}P, external 85% H_3PO_4; ^{195}Pt, external 0.1 M $Na_2[PtCl_6]$ in H_2O; ^{109}Ag, $AgClO_4$ in H_2O extrapolated to infinite dilution. A positive sign denotes a shift downfield from the reference. The simulation of the spectra was carried out using the Program PANIC provided by Bruker GmbH. The C, H, and P analyses were carried out by the Microanalytical Laboratory of the Organic Chemistry Laboratory of the ETH, while the metal analyses were obtained by ICP atomic emission spectroscopy carried out by the Analytical Section of the Inorganic Chemistry Laboratory of the ETH.

Syntheses. *trans*-$[PtH(C_6H_5)(PEt_3)_2]$,[17] *trans*-$[PtH(C_6F_5)(PEt_3)_2]$,[18] *trans*-$[PtH(C_6Cl_5)(PEt_3)_2]$,[19] *trans*-$[PtH(C_6Cl_5)(PMe_3)_2]$,[20] and $[Pt(PMe_3)_4]$[21] were prepared as described in the appropriate references. $AgCF_3SO_3$ was purchased from Fluka AG and used without further purification. The other compounds were prepared as described below.

***trans*-$[PtBr(C_6F_5)(PMe_3)_2]$.** Neat C_6F_5Br (2 g, 8.10 mmol) was added dropwise to a stirred solution of $[Pt(PMe_3)_4]$ (3.07 g, 6.15 mmol) in 20 mL of Et_2O, which had been precooled to −80 °C. A white precipitate formed immediately. The suspension was allowed to warm to room temperature and stirred for another 1 h. The solvent and excess C_6F_5Br were distilled off under vacuum, the residue was extracted with Et_2O, and the solvent was evaporated to dryness. The crude product was recrystallized from Et_2O. Yield: 85%. Mp: 199 °C. Anal. Calcd for $C_{12}H_{18}BrF_5P_2Pt$: C, 24.26; H, 3.05; Br, 13.45. Found: C, 24.72; H, 3.12; Br, 14.13.

***trans*-$[PtH(C_6F_5)(PMe_3)_2]$ (3a).** Solid $NaBH_4$ (0.5 g, 13 mmol) was gradually added to a stirred solution of *trans*-$[PtBr(C_6F_5)(PMe_3)_2]$ (1.81 g, 3.05 mmol) in $EtOH/H_2O$ (20 mL, 5:1) which had been precooled to 0 °C. The solution was allowed to warm to room temperature, and stirring was continued for 3 h after gas evolution had ceased. The product was precipitated by the addition of water and filtered off. The solid was extracted with CH_2Cl_2, the solution filtered off, and the residue dried under vacuum. The crude product thus obtained was recrystallized from acetone. Yield: 86%. Dec pt: 150 °C. Anal. Calcd for $C_{12}H_{19}F_5P_2Pt$: C, 27.97; H, 3.72. Found: C, 28.11; H, 3.59.

$[(PMe_3)_2(C_6F_5)Pt(\mu\text{-}H)Ag(\mu\text{-}H)Pt(C_6F_5)(PMe_3)_2](CF_3SO_3)$ ([2a]-(CF_3SO_3)). Solid $AgCF_3SO_3$ (0.050 g, 0.19 mmol) was added to a solution of *trans*-$[PtH(C_6F_5)(PMe_3)_2]$ (0.206 g, 0.40 mmol) in 15 mL of diethyl ether. The suspension was stirred for 4 h and the white precipitate formed filtered off. The solid was redissolved in the minimum amount of CH_2Cl_2. A layer of pentane was floated over this solution, and the container was placed in a refrigerator at −20 °C. The colorless crystals thus formed were filtered off and dried. Yield: 62%. Dec: ca. 120 °C. Anal. Calcd for $C_{25}H_{38}AgF_{13}O_3P_4Pt_2S$: C, 23.32; H, 2.97. Found: C, 23.68; H, 3.06.

$[(PMe_3)_2(C_6Cl_5)Pt(\mu\text{-}H)Ag(\mu\text{-}H)Pt(C_6Cl_5)(PMe_3)_2](CF_3SO_3)$ ([2b](CF$_3$SO$_3$)) was prepared as described above from $AgCF_3SO_3$ (0.050 g, 0.19 mmol) and *trans*-$[PtH(C_6Cl_5)(PMe_3)_2$ (0.239 g, 0.40 mmol). Yield: 66%. Dec: ca. 105 °C. Anal. Calcd for

(13) Barrow, M.; Bürgi, H.-B.; Camalli, M.; Caruso, F.; Fischer, E.; Venanzi, L. M.; Zambonelli, L. *Inorg. Chem.* **1983**, *22*, 2356.
(14) Camalli, M.; Caruso, F.; Chaloupka, S.; Venanzi, L. M. *Helv. Chim. Acta* **1988**, *71*, 703.
(15) (a) Robertson, G. B.; Tucker, P. A. *Acta Crystallogr.* **1983**, *C39*, 1354. (b) Crespo, M.; Sales, J.; Solans, X.; Font Altaba, M. *J. Chem. Soc., Dalton Trans.* **1988**, 1617.
(16) From molecular force field fitting of microwave data: Cook, R. L.; De Lucia, F. C.; Helmlinger, P. *J. Mol. Spectrosc.* **1974**, *53*, 62.
(17) Arnold, D. P.; Bennett, M. A. *Inorg. Chem.* **1984**, *23*, 2117.
(18) Fornies, J.; Grenn, M.; Spencer, J. L.; Stone, F. G. A. *J. Chem. Soc., Dalton Trans.* **1977**, 1006.
(19) Carmona, D.; Chaloupka, S.; Jans, J.; Thouvenot, R.; Venanzi, L. M. *J. Organomet. Chem.* **1984**, *275*, 303.
(20) McGilligan, B. S.; Venanzi, L. M.; Wolfer, M. *Organometallics* **1987**, *6*, 946.
(21) Mann, B. E.; Musco, A. *J. Chem. Soc., Dalton Trans.* **1980**, 776.

Table III. Crystal Data and Collection and Refinement Parameters for $[(PEt_3)_2(C_6Cl_5)Pt(\mu\text{-}H)Ag(\mu\text{-}H)Pt(C_6Cl_5)(PEt_3)_2](CF_3SO_3)$ ([**2e**](CF_3SO_3)) and $[(PEt_3)_2(C_6Cl_5)Pt(\mu\text{-}H)Ag(H_2O)](CF_3SO_3)$ ([**5e**](CF_3SO_3))

	[**2e**](CF_3SO_3)	[**5e**](CF_3SO_3)	
	X-ray	X-ray	neutron
formula	$C_{37}H_{62}AgCl_{10}F_3O_3P_4Pt_2S$	$C_{19}H_{33}Cl_5F_3O_4P_2PtS$	
fw	1620.42	956.69	
data collection T (K)	298	298	24 (1)
cryst system	triclinic	triclinic	triclinic
a (Å)	13.853 (3)	8.739 (4)	8.581 (2)
b (Å)	14.214 (2)	12.080 (18)	12.053 (3)
c (Å)	15.611 (3)	15.870 (11)	15.519 (3)
α (deg)	94.64 (2)	86.50 (9)	87.86 (2)
β (deg)	90.48 (2)	74.85 (7)	73.55 (2)
γ (deg)	110.39 (2)	82.90 (8)	81.76 (2)
V (Å^3)	2869.7	1603.3	1523
ρ_{calcd} (g cm^{-3})	1.875	1.980	2.105
Z	2	2	2
space group	$P\bar{1}$	$P\bar{1}$	$P\bar{1}$
cryst dimens (mm)	0.15 × 0.20 × 0.30	0.3 × 0.2 × 0.08	1.50 × 0.36 × 1.50
radiation λ (Å)	0.710 69 (graphite monochromated, Mo Kα)	0.710 69 (graphite monochromated, Mo Kα)	1.158 82 (7) (Ge, 220 reflct plane)
μ (cm^{-1})	56.256	59.180	2.108
transm factors: max, min	0.999, 0.774	0.998, 0.521	0.914, 0.664
scan mode	$\omega/2\theta$	$\omega/2\theta$	$\omega/2\theta$
max scan speed (deg min^{-1})	10.05	10.05	
scan width (deg)	1.0 + 0.35 tan θ	1.20 + 0.35 tan θ	3.2 for 0.045 < (sin θ)/λ ≤ 0.431 Å^{-1} 3.2–5.2 for 0.431 ≤ (sin θ)/λ ≤ 0.610 Å^{-1}
max counting time (s)	60	60	
prescan rejection lim	0.5 (2σ)	0.5 (2σ)	
prescan acceptance lim	0.03 (33σ)	0.03 (33σ)	
bkgd time	0.5 × scan time	0.5 × scan time	
horiz receiving aperture (mm)	1.90 + tan θ	1.95 + tan θ	12.0
vert receiving aperture (mm)	4.0	4.0	12.0
measd reflecns	$\pm h,\pm k,+l$	$\pm h,\pm k,+l$	$+h,\pm k,\pm l$
(sin θ)/λ range (Å^{-1})	0.054–0.539	0.061–0.539	0.045–0.610
no. of data collected	7090	5250	6619
no. of independent data			5799
no. of data used in the refinement (n_o)	5235 ($F_o \geq 2.5\sigma(F_o)$)	3112 ($F_o \geq 2.0\sigma(F_o)$)	5572
no. of parameters varied (n_v)	369	272	624
R_{av} (agreement on averaging)[a]			0.024
R[b]	0.049	0.062	0.081
R_w[c]	0.057	0.082	0.087
GOF(S)[d]	1.51	2.39	1.63

[a] $R_{av} = \sum_i^n |F_o^2| - (F_o)_i^2 / \sum_n F_o^2$. [b] R(X-ray) = $\sum||F_o| - 1/k|F_c||/\sum|F_o|$; R(neutron) = $\sum|(F_o^2 - k^2F_c^2)|/\sum|F_o^2|$. [c] R_w(X-ray) = $[\sum w(|F_o| - 1/k|F_c|)^2/\sum w|F_o|^2]^{1/2}$; R_w(neutron) = $[\sum w(F_o^2 - k^2F_c^2)^2/\sum wF_o^4]^{1/2}$. [d] S(X-ray) = $[\sum w(|F_o| - (1/k)|F_c|)^2/(n_o - n_v)]^{1/2}$; S(neutron) = $[\sum w(F_o^2 - k^2F_c^2)^2/(n_o - n_v)]^{1/2}$.

$C_{25}H_{38}AgCl_{10}F_3O_3P_4Pt_2S$: C, 20.68; H, 2.64. Found: C, 20.32; H, 2.94.

$[(PEt_3)_2(C_6H_5)Pt(\mu\text{-}H)Ag(\mu\text{-}H)Pt(C_6H_5)(PEt_3)_2](CF_3SO_3)$ ([**2c**](CF_3SO_3)). All operations described below were carried out at −70 °C. Solid $AgCF_3SO_3$ (0.076 g, 0.3 mmol) was added to a precooled stirred solution of *trans*-$[PtH(C_6H_5)(PEt_3)_2]$ (0.303 g, 0.6 mmol) in ca. 5 mL of diethyl ether. Stirring was continued, and the white precipitate formed was filtered off and dried under high vacuum. Yield: 58%. This compound is particularly light-sensitive and should also be stored at −70 °C. Satisfactory microanalytical data for this compound could not be obtained because it partially decomposed during transfer to the apparatus.

$[(PEt_3)_2(C_6F_5)Pt(\mu\text{-}H)Ag(\mu\text{-}H)Pt(C_6F_5)(PEt_3)_2](CF_3SO_3)$ ([**2d**](CF_3SO_3)) was prepared as described above from $AgCF_3SO_3$ (0.050 g, 0.19 mmol) and *trans*-$[PtH(C_6F_5)(PEt_3)_2]$ (0.240 g, 0.40 mmol). Yield: 0.169 g, 58%. Dec: ca. 130 °C. Anal. Calcd for $C_{37}H_{62}AgF_{13}O_3P_4Pt_2S$: C, 30.52; H, 4.29. Found: C, 30.94; H, 4.73.

$[(PEt_3)_2(C_6Cl_5)Pt(\mu\text{-}H)Ag(\mu\text{-}H)Pt(C_6Cl_5)(PEt_3)_2](CF_3SO_3)$ ([**2e**](CF_3SO_3)) was prepared as described above from $AgCF_3SO_3$ (0.034 g, 0.132 mmol) and *trans*-$[PtH(C_6Cl_5)(PEt_3)_2]$ (0.180 g, 0.264 mmol). Yield: 61%. Dec: ca. 120 °C. Anal. Calcd for $C_{37}H_{62}AgCl_{10}F_3O_3P_4Pt_2S$: C, 27.42; H, 3.86. Found: C, 27.69; H, 3.88.

$[(PEt_3)_2(C_6Cl_5)Pt(\mu\text{-}H)Ag(H_2O)](CF_3SO_3)$ ([**5e**](CF_3SO_3)). Solid $AgCF_3SO_3$ (0.034 g, 0.132 mmol) was added to a reagent grade Et_2O (2 mL) solution of *trans*-$[PtH(C_6Cl_5)(PEt_3)_2]$ (0.090 g, 0.132 mmol), and the suspension was stirred for 1 h. The solution was evaporated to dryness under reduced pressure. The colorless residue was recrystallized by dissolving it in CH_2Cl_2, floating a layer of pentane over the solution, and placing the flask in a refrigerator at −20 °C. Yield: 62%. Dec: ca. 132 °C. Anal. Calcd for $C_{19}H_{33}Cl_5F_3O_4P_2PtS$: C, 23.85; H, 3.48. Found: C, 24.17; H, 3.29.

X-ray Structure Determination of $[(PEt_3)_2(C_6Cl_5)Pt(\mu\text{-}H)Ag(\mu\text{-}H)Pt(C_6Cl_5)(PEt_3)_2](CF_3SO_3)$ ([**2e**](CF_3SO_3)). White, air-stable prismatic crystals were obtained by slow diffusion of pentane into a CH_2Cl_2 solution of the crude product. For data collection, a crystal was mounted on a glass fiber at a random orientation on a Nonius CAD4 diffractometer. Cell constants were obtained by a least-squares fit of the 2θ values of 25 reflections (10° ≤ θ ≤ 18°) using the CAD4 centering routines.[18] Crystallographic and data collection parameters are given in Table III. Data were collected at variable scan speed to obtain constant statistical precision on the collected intensities. The stability of the crystal and of the experimental conditions was checked every hour using three reflections evenly distributed in reciprocal space, while the orientation was monitored every 300 reflections by centering three standards. Data were corrected for Lorentz and polarization factors and for the decay of the crystal (correction factors in the range 0.966–1.167). An empirical absorption correction was also applied using the azimuthal (Ψ) scans of three reflections at high χ angle (86° < χ < 88°). The SDP system of programs was used for both the data reduction and the absorption correction.[22] The standard deviations of the intensities were calculated in terms of counting statistics, and I_{net} = 0.0 was given to those reflections having negative net intensities. Only those reflections with $F_o \geq 2.0\sigma(F)$ were considered as observed and used for the solution and refinement of the structure. The structure was solved by Patterson and Fourier methods and refined by block-diagonal least-squares techniques[23] minimizing the function $[\sum w(|F_o| - k|F_c|)^2]$ with weights obtained from a Cruickshank scheme[24] by demanding that no systematic trend be present

(22) *Enraf-Nonius Structure Determination Package, SDP*; Enraf-Nonius: Delft, The Netherlands, 1980.

(23) Albinati, A.; Brückner, S. *Acta Crystallogr. Sect. B* **1978**, *B34*, 3390 and references quoted therein.

(24) Cruickshank, D. W. J. In *Computing Methods in Crystallography*; Ahmed, A., Ed.; Munksgaard: Copenhagen, 1970.

in the weights with $|F_o|$ or $(\sin\theta)/\lambda$. No extinction correction was applied. The scattering factors used, corrected for anomalous dispersion, were taken from tabulated values.[25]

Anisotropic temperature factors for the Pt, Ag, Cl, and P atoms and isotropic temperature factors for the all the other atoms were used. Upon convergence (no parameter shift > $0.2\sigma(p)$), a difference Fourier map showed two peaks consistent with the expected positions for the bridging ligands. The inclusion of these two hydrides in the final refinement led to convergence and an acceptable geometry, even with the expected high standard deviations. The final positional and thermal parameters are obtainable as indicated in the supplementary material.

X-ray Structure Determination of $[(PEt_3)_2(C_6Cl_5)Pt(\mu\text{-}H)Ag(H_2O)](CF_3SO_3)$ ([5e](CF_3SO_3)). Crystals of [5e](CF_3SO_3), suitable for X-ray analysis, were obtained by recrystallizing the crude product from CH_2Cl_2/pentane. A platelike crystal was used as above for space group and cell parameter determination and data collection. Accurate cell constants were obtained by a least-squares fit of the 2θ values of 25 reflections ($10° \le \theta \le 19°$); crystallographic and data collection parameters are given in Table III. The data collection and the subsequent data reduction were carried out as described above, by using for the azimuthal scans three reflections having χ angles > 81° and considering as observed those reflections with $F_o > 2.5\sigma(F)$. Anisotropic thermal parameters were used for the Pt, Ag, P, and Cl atoms as well as those of $CF_3SO_3^-$ and the phenyl ring, while isotropic parameters were used for the remaining atoms. It proved impossible to locate the hydride ligand unambiguously by inspection of difference Fourier maps that were calculated with a limited data set ($(\sin\theta)/\lambda$ cutoff 0.32 Å^{-1}). An attempt to locate possible positions for the hydrogen ligands using a potential energy search with the program Hydex[26] gave two minima of approximately equal energy symmetrically located between the Ag and Pt atoms. Subsequently, neutron diffraction showed the presence of a single bridging hydride ligand. The final positional parameters are listed in Table S4 and the thermal parameters are listed in Table S2 (supplementary material).

Neutron Diffraction Structure Determination of [5e](CF_3SO_3). A colorless platelike crystal with a volume of 1.2 mm^3 and weight of 2.4 mg was mounted on an Al pin approximately along the crystallographic 122 axis using halocarbon grease. The mount was sealed under a He atmosphere in an Al can attached to a closed-cycle He refrigerator,[27] which was placed on a four-cycle diffractometer[28,29] at the Brookhaven High Flux Beam Reactor. The measurements were carried out at a temperature of 24 K. Calibration of the Ge(220)-monochromated neutron beam was carried out with a KBr crystal (a_0 = 6.6000 Å at T = 298 K),[30] yielding a value of λ = 1.158 82 (7) Å. A least-squares fit of the $\sin^2\theta$ values of 18 reflections in the range $0.309 < (\sin\theta)/\lambda < 0.489$ Å^{-1} gave the unit-cell parameters listed in Table III.

Intensity data were collected in the $\omega/2\theta$ step-scan mode. The $+h,\pm k,\pm l$ hemisphere of reciprocal space was scanned, with a constant scan of $\Delta 2\theta = 3.2°$ (80 steps) for the low-angle region ($0.045 \le (\sin\theta)/\lambda < 0.431$ Å^{-1}). The variable scans for the high-angle region ($0.431 \le (\sin\theta)/\lambda \le 0.610$ Å^{-1}) were determined by the dispersion relation $\Delta 2\theta$ (deg) = 0.5 + 4.7 tan θ. The total width of any scan was adjusted to give between 60 and 90 steps. The duration of each step was about 4 s and depended on a constant monitor count of the incident beam. Three reference intensities were measured after every 100 reflections; analysis[31] of these reference intensities showed no significant variation throughout the course of the experiment.

Backgrounds were computed on the basis of the counts recorded for 10% of the steps at either end of each scan, and the resulting integrated intensities were then corrected for Lorentz and absorption effects. The latter correction employed a numerical integration over a Gaussian grid of 16 × 12 × 8 points relative to the reciprocal cell vectors. Averaging of identical or Friedel-related data yielded 5799 unique squared structure factors, of which 227 were judged to be contaminated by scattering from the Al cryostat and were omitted from the structure refinement.

Starting values for the coordinates of non-hydrogen atoms were taken from the X-ray results, and all hydrogen atoms were located in a series of difference Fourier syntheses alternated with least-squares refinement including isotropic thermal parameters. The complete structure model was refined by a full-matrix least-squares procedure, with anisotropic thermal parameters for all 69 atoms and by varying a total of 624 parameters, including the occupancy of the water molecule. A type I isotropic extinction correction[32] was employed, and the extinction parameters converged to g = 1294 (201), corresponding to a mosaic spread of a 45″ arc.

The quantity $\sum w(F_o^2 - k^2F_c^2)^2$, with weights $w = [\sigma^2(F_o^2)]^{-1}$ and $\sigma^2(F_o^2) = [\sigma_{count}^2(F_o^2) + (0.017F_o^2)^2]$, was minimized in the least-squares procedure, at the completion of which all parameter shift/error values were 0.06 or less. The final difference Fourier synthesis produced no significant features (largest positive residual < 8% of a C atom peak). Indices of fit are presented in Table III. Final atomic positional and equivalent isotropic thermal parameters (Table S5), anisotropic thermal parameters (Table S3), and observed and calculated squared structure factors and esd's (Table S6) are provided as supplementary material.

Neutron scattering lengths were taken from a compilation by Koester et al.[33] All calculations were performed on a μVAX computer using programs described by Lundgren.[34]

Acknowledgment. M.K.W. carried out the work during the tenure of a research fellowship from the Swiss National Science Foundation, while A.A. and T.F.K. acknowledge the support of NATO Grant 85/068. The neutron diffraction study was carried out at Brookhaven National Laboratory under Contract DE-AC02-76CH00016 with the U.S. Department of Energy, Division of Chemical Sciences, Office of Basic Energy Sciences.

Supplementary Material Available: For [5e](CF_3SO_3), Tables S1–S5, giving extended lists of bond lengths and angles (neutron data), anisotropic thermal parameters (X-ray data), anisotropic thermal parameters (neutron data), final positional parameters (X-ray data), and final atomic positional and equivalent isotropic thermal parameters (neutron data) (47 pages); Table S6, listing observed and calculated squared structure factors (neutron data) (34 pages). Ordering information is given on any current masthead page. For [2e](CF_3SO_3), Figure S1, an ORTEP plot of the cation **2e** with the full numbering scheme, and tables of final positional and thermal parameters, observed and calculated structure factors, and an extensive list of interatomic distances and angles are available upon request from the Fachinformationszentrum Energie, Physik, Mathematik GmbH, D-7514 Eggenstein-Leopoldshafen 2, Germany, on quoting the depository number CSD-52845, the names of the authors, and the journal citation.[3]

(25) *International Tables for X-ray Crystallography*; Kynoch Press: Birmingham, England, 1974; Vol. IV.
(26) Orpen, A. G. *J. Chem. Soc., Dalton Trans.* **1980**, 2509.
(27) Air Products and Chemicals, Inc.; DISPLEX Model CS-202.
(28) McMullan, R. K.; Andrews, L. C.; Koetzle, T. F.; Reidinger, F.; Thomas, R.; Williams, G. J. B. NEXDAS, Neutron and X-Ray Data Acquisition System. Unpublished work.
(29) Dimmler, D. G.; Greenlaw, N.; Kelley, M. A.; Potter, D. W.; Rankowitz, S.; Stubblefield, F. W. *IEEE Trans. Nucl. Sci.* **1976**, *23*, 298.
(30) Donnay, J. D. H., Ondik, H. M., Eds. *Crystal Data Determinative Tables*, 3rd ed.; U.S. Department of Commerce and Joint Committee on Powder Diffraction Standards: Washington, DC, 1973; Vol. 2, p C-164.
(31) McCandlish, L. E.; Stout, G. H.; Andrews, L. C. *Acta Crystallogr., Sect. A* **1975**, *A31*, 245.
(32) Becker, P. J.; Coppens, P. *Acta Crystallogr., Sect. A* **1975**, *A31*, 417.
(33) Koester, L.; Rauch, H.; Herkens, M.; Schröder, K. *KFA Report Jül-1755*; KFA Jülich GmBH: FRG, 1981.
(34) Lundgren, J.-O. Report UUIC-913-4-05; Institute of Chemistry, University of Uppsala: Uppsala, Sweden, 1983.